

As is well known, atomic membranes are obtained by bombarding thin polymeric films [mainly polyethylene terephthalate (PETP)] by heavy ions followed by chemical treatment [1]. A feature of these filtration materials is pore shape which is close to cylindrical, uniformity of the structure, and very low dispersion of pore size.

The spectrum of application for atomic membranes is quite extensive. By using them, it is possible to solve a whole series of problems in science and technology. A considerable proportion of atomic membranes are used for separating suspensions, liquid and gas mixtures, fine purification of water and air, etc., i.e., in those processes where membrane elements are subject to pressure drops.

It is well known that action on a membrane of a certain force (pressure) leads to occurrence in the polymer matrix of internal stresses. Since an atomic membrane is a porous body, then stresses in it are not distributed uniformly. Internal stress concentrations will be observed close to pores [2] which may serve as the reason for unstable operation of membrane elements. There is practically no work devoted to studying the behavior of atomic membranes in a loaded condition.

In this work an attempt is made to a certain extent to clarify processes occurring during loading of an atomic PETP membrane by a pressure difference. A method of gasdynamic monitoring for pore geometry of a cellular-type membrane is taken as a basis [3].

Deformation Properties of Partially Crystalline PETP. In order to prepare PETP atomic membranes it is normal to use partially crystalline (degree of crystallinity ~50%) biaxially oriented film 10  $\mu\text{m}$  thick according to GOST 24234-80.

The mechanical properties of partially crystalline (crystalline) polymers are characterized by the stress  $\sigma$ -strain  $\epsilon$  curve. The typical form of this relationship is presented in Fig. 1, and it is almost similar to the corresponding curve for glassy polymers.

The specific form of the relationship  $\sigma = f(\epsilon)$  for the polymeric material of the membrane is governed by a whole series of factors: physical state of the specimen, its structural features, molecular weight, loading conditions, geometrical dimensions, deformation temperature, etc. [4, 5]. The effect of these factors may also explain the considerable scatter of PETP-film characteristics in the literature [6].

The mechanical properties of polymeric materials are normally determined in different machines both in uniaxial and biaxial tension. Biaxial tension is realized by a scheme shown in Fig. 2, and strain is the ratio of increase in area of specimen surface  $\Delta S$  to the area of the original specimen  $S$ :  $\epsilon = \Delta S/S \cdot 100 = (H/R_0)^2 \cdot 100$ .

Let specimens of atomic membranes with pores of strictly cylindrical shape, the distance between which is considerably greater than pore size, be subjected to biaxial tension. Then, according to [7], stresses occurring close to a pore may be expressed in the form

$$\sigma_{rr} = \sigma_0 \left( 1 - \frac{R_p^2}{r^2} \right), \quad \sigma_{\varphi\varphi} = \sigma_0 \left( 1 + \frac{R_p^2}{r^2} \right), \quad \sigma_{zz} \simeq \sigma_{0z} \quad (1)$$

where  $\sigma_{rr}$ ,  $\sigma_{\varphi\varphi}$ , and  $\sigma_{zz}$  are stressed in a cylindrical coordinate system with axis  $z$  along the pore axis;  $R_p$  is pore radius;  $r$  is radial coordinate;  $\sigma_0$  is stress in the film at a distance from pores.

It follows from (1) that in the local vicinity of a pore ( $r \approx 1-3 R_p$ ) stresses  $\sigma_{\varphi\varphi}$  exceed  $\sigma_0$ . This means a situation is possible when  $\sigma_0$  will be less than stresses of induced

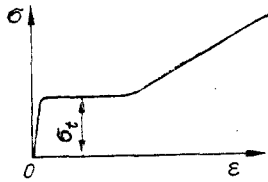


Fig. 1

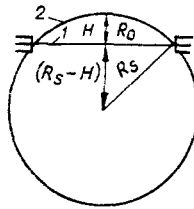


Fig. 2

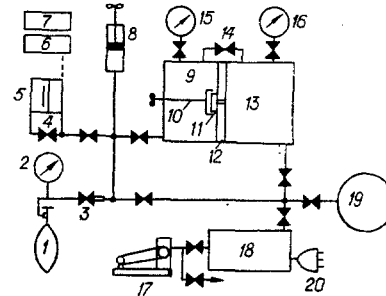


Fig. 3

polymer elasticity  $\sigma_t$ , and in regions around pores  $\sigma_{\phi\phi}$  appears to be of the order or exceeds  $\sigma_t$  (with  $r = R_p$ ,  $\sigma_{\phi\phi} = 2\sigma_0$ ). In this case strains in the polymer material of a membrane will be insignificant (on the basis of observing Hooke's law), and pore radius is markedly increased due to significant strains in regions surrounding pores. The mechanism described is not excluded during atomic membrane operation in a loaded state and it requires experimental study.

**Experimental Technique and Procedure for Performing Measurement.** A study of the deformation of pores occurring in atomic membranes loaded by a pressure difference was carried out by a gasdynamic method in equipment (Fig. 3) which consists of the following main parts: a system for admitting gases (cylinder with pure gas 1, manometer 2, and leakage valve 3); a system for measuring flow rate (bypass valve 4 of differential micromanometer 5 with output to an LC-generator 6 and a digital frequency meter 7, flowmeter 8 with commutating valves); working chamber with a filter holder (gas supply chamber 9, stopper 10 for the filter holder with the atomic membrane 11, flange 12, low-pressure chamber 13, valve 14, and manometer (vacuum meters 15 and 16 with commutating valves); vacuum system (backing pump 17 connected with cylinder 18, adsorption pump 19, and vacuum gauge 20).

The working chamber is constructed in the form of two vessels 9 and 13 held in a central flange with the filter holder in which the atomic membrane is held between two disks with coaxial vacuum-tight openings. The gasdynamic permeability of atomic membranes was measured by the steady flow method, as follows. After short-term evacuation by the backing pump, the working chamber, and also the system for measuring flow rate, was evacuated to a pressure of  $\sim 10^{-2}$  Pa by the adsorption pump. After evacuation pure gas from the cylinder was fed slowly by the leakage valve to both vessels of the working chamber and the system for measuring flow rate to pressure  $p_2$  which was recorded by the specimen manometer (vacuum gauge) 16 with an error of  $\sim 1.5\%$ . Then the stopper of the filter holder and bypass valve connecting vessels 9 and 13 were closed. Then the volume of the working chamber and the system for measuring flow rate were filled with gas to pressure  $p_1$  which was recorded by a manometer vacuum gauge 15 with an error not exceeding  $\sim 1.5\%$ . The bypass valve of the differential micromanometer with a sensitivity of  $\sim 4 \cdot 10^{-3}$  Pa/Hz was shut off (operating principle similar to that given in [8]) and the "zero" frequency of the generator with its thermal drift was recorded.

A flow of gas through the membrane under the action of the pressure difference  $\Delta p = p_1 - p_2$  is organized by opening the stopper of the filter holder. The volume of chamber 13 is quite large ( $\sim 1500$  cm<sup>3</sup>) and, therefore, the change in pressure during the time of measuring gas flow rate ( $\sim 50$ - $100$  sec) may be ignored. Pressure in vessel 9 was maintained at a constant level by moving the piston of the flowmeter according to the control signal of the micromanometer generator with an error of not more than 0.5%. Gas flow rate through the membrane in this case was determined as  $Q = (\pi D^2/4) \Delta l / \Delta t$  ( $\Delta l$  is piston displacement of the flowmeter in time  $\Delta t$ ,  $D$  is piston diameter).

In order to interpret test data it is more convenient to operate with values of total flow rate  $Q^*$  and relative total flow rate  $\omega$ :  $Q^* = Q p_1 / \Delta p$ ,  $\omega = (Q^* / Q_{Xe}^*) (M / M_{Xe})^{0.5}$  ( $Q^*$  and  $Q_{Xe}^*$  are total flow rate of the gas used and total free-molecular flow rate of Xe,  $M$  and  $M_{Xe}$  are molecular weight of the test gas and xenon).

In test dependences were obtained for  $\omega$  and  $Q^*$  on the rarefaction parameter  $\delta$  connected with Knudsen number  $Kn$ :  $\delta = (\sqrt{\pi}/2) (R_p / \lambda) = (\sqrt{\pi}/2) (1 / Kn)$  ( $\lambda$  is average length to free travel for a gas molecule).

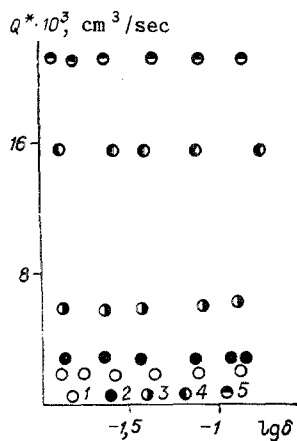


Fig. 4

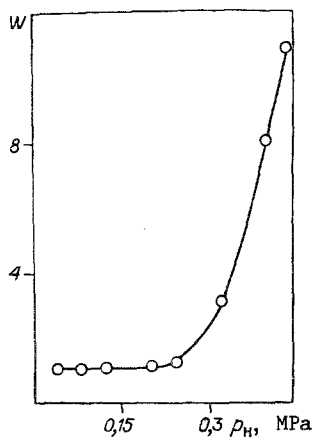


Fig. 5

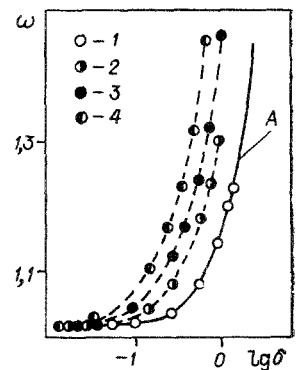


Fig. 6

TABLE 1

Specimen number	$2R_p$ , nm	$n$ , $\text{cm}^{-2}$	$L$ , $\mu\text{m}$	$s$ , $\text{cm}^2$
1	$13,0 \pm 0,6$	$(3,0 \pm 0,5) \cdot 10^8$	10	$0,196 \pm 0,003$
2	$37,8 \pm 1,6$	$(1,0 \pm 0,15) \cdot 10^7$	10	$0,95 \pm 0,03$
3	$118 \pm 6$	$(1,01 \pm 0,14) \cdot 10^7$	10	$0,95 \pm 0,03$

Deformation changes occurring in an atomic membrane with loading by pressure  $p_H$  may be detected if compared with experimental relationships  $Q^* = f(\log \delta)$  [or  $\omega = f(\log \delta)$ ] before and after loading.

Loading of a membrane was carried out at rate of  $\sim 10^4$  Pa/sec by supplying gas through the leakage valve into the vessel of working chamber 9 with an open stopper and closed bypass valve.

The pressure in vessel 13 was always of the order of  $10 \cdot 10^{-1}$  Pa. A specimen was held in the loaded condition for 5 min. As is well known, in stretched film after removing the load there is an internal stress relaxation process. Tests showed that the rate of relaxation becomes insignificant after 1-1.5 h from the instant of specimen unloading. Therefore, after removing the pressure drop specimens were held in a vacuum for 2 h.

Experimental Results and Discussion. Studies were carried out on three specimens of PETP-film atomic membranes whose geometric characteristics are given in Table 1.

Presented in Fig. 4 are experimental relationships  $Q^* = f(\log \delta)$ , measured after successive loading of specimen 1 with pressures 0.04, 0.23, 0.32, 0.4, and 0.44 MPa (points 1-5). All of the measurements were carried out at room temperature (296 K). Argon with a purity not worse than 99.9% was chosen as the operating gas. Test data for gas flow rate was obtained with a pressure difference in the range from 4 to 40 kPa. Deformation processes in the polymeric matrix of the membrane may be ignored, and thus it is possible to assume that the membrane was conditionally unloaded. The systematic error in determining  $Q^*$  did not exceed 2%. In Fig. 4 all of the relationships  $Q^* = f(\log \delta)$  have a typical form of a Knudsen plateau which points to the freely molecular flow regime for the gas ( $Kn \gg 1$ ). With an increase in loading pressure  $p_H$  a marked increase is observed in the values of  $Q^*$ . This is shown more clearly in Fig. 5. The value of  $W = Q^*/Q_0^*$  characterizes the ratio of relative Knudsen gas flow rate  $Q^*$  measured after loading the membrane with pressure  $p_H$  to flow rate  $Q_0^*$  corresponding to pressure  $p_H = 0.04$  MPa. Difference of  $W$  from unity becomes marked on exceeding pressure  $p_H \sim 0.25$  MPa, and with  $p_H = 0.44$  MPa it reaches  $\sim 1000\%$ . According to the specification the maximum relative strain for PETP film should be about 7-10% with  $p_H = 0.44$  MPa. Visual observation of atomic deflection in the filter-holder at the pressure mentioned established that the relative strain for the area did not exceed 15%. Calculations show that an increase in through pore cross section by 10% may only lead to a 15% increase in flow rate. In tests the increase in  $Q^*$  is observed by an order of magnitude which is apparently connected with occurrence of considerable ( $\sim 100$ - $200\%$ ) polymer strain in regions

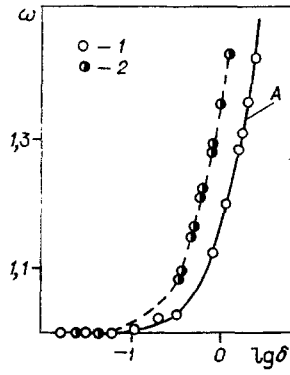


Fig. 7

TABLE 2

Specimen number	$p_H$ , MPa	$R_p$ , nm	
		gas dynamic	electron microscope
2	0	18,9±0,8	27±3
	0,24	33,5±1,5	—
	0,32	46,5±2,1	—
	0,4	63,0±2,6	68±17
3	0	59±3	63±13
	0,44	119±6	125±15

TABLE 3

Specimen number	$p_H$ , MPa	$Q^*/Q_0^*$	$R_p/R_0 p^0$	
			from (2)	gas dynamic
2	0,24	5,41±0,10	1,751±0,023	1,77±0,11
	0,32	14,71±0,20	2,451±0,023	2,46±0,16
	0,4	36,3±0,3	3,31±0,03	3,33±0,22
3	0,44	8,49±0,20	2,041±0,021	2,02±0,10

directly adjacent to pores. The reason for the phenomenon observed may be connected with reaching (or exceeding) stresses  $\sigma_{\varphi\varphi}$  in the space around pores stresses of polymer-induced plasticity  $\sigma_t$ . In order to be sure of this it is sufficient to estimate stresses occurring in specimen 1 with "critical" loading pressure  $p_H \sim 0.25$  MPa on the basis of the scheme in Fig. 2 and Hooke's law for a uniformly extended plate  $\Delta S/S = \sigma_0 [2(1 - \mu)/E] \approx H^2/R_0^2$  ( $E$  is elasticity modulus) and assuming that  $H^2/R_0^2 \ll 1$  it is easy to obtain the correlation of

stresses in the film with loading pressure  $\sigma_0 = \left( \frac{E p_H^2}{32(1 - \mu)} \frac{R_0^2}{L^2} \right)^{1/3}$  ( $L$  is membrane thickness).

By taking Poisson's ratio  $\mu = 0.25$ ,  $p_H = 0.25$  MPa,  $R_0/L = 250$ ,  $E = 4000$  MPa, we find  $\sigma_{\varphi\varphi} = 2\sigma_0 \approx 180$  MPa, which in fact falls in the region of values of  $\sigma_t$  for PETP approximately equal to the strength limit.

In order to check whether the observed value of freely molecular gas flow rate is connected with occurrence of any cracks and discontinuities in the film during its extension, direct measurements of pore radius were carried out in membranes 2 and 3 before and after loading by two independent methods.

Presented in Figs. 6 and 7 are relationships of the type  $\omega = f(\log \delta)$  obtained by a gas dynamic method, and point 1 corresponds to an unloaded specimen (operating pressure difference did not exceed 0.04 MPa). From the condition of best conformity of experimental values

with empirical relationship A obtained in membrane specimens and values of  $n$  and  $R_p$ , initial effective gas pore radii were determined (procedure similar to that given in [3]).

Experimental curves  $\omega = f(\log \delta)$  (points 2-4 in Fig. 6) were plotted for specimen 2 previously loaded by pressures 0.24, 0.32, and 0.4 MPa, respectively. Similarly, for specimen 3 (point 2 in Fig. 7) relationship  $\omega = f(\log \delta)$  was found for  $p_H = 0.44$  MPa (the relative strain for PETP film was ~25-30%). Parameter  $\delta$  in all of the cases was calculated from the original average pore radius for a membrane in the unloaded state. With this choice of  $\delta$  in Figs. 6 and 7 shifts are clearly observed (to the left along the abscissa axis) for relationship  $\omega = f(\log \delta)$  of loaded specimens with respect to unloaded specimens. This points to an increase in through pore cross sections for atomic membranes. Quantitatively pore-size measurements may be determined by selecting average radius  $R_p$  (and, consequently, the calculation of parameter  $\delta$ ) from the condition of best conformity of curves 2-4 with empirical relationship A. The data obtained for pore radius measurements in specimens with loading are given in Table 2. The error of gasdynamic determination of pore radius did not exceed 5%. Apart from gasdynamic tracing of membrane pore expansion during loading, an estimate was made of inlet pore cross section by the method of electron microscopy. Surface dimensions to pores were estimated by means of a Japanese JEDL scanning electron microscope JSM-840.

Comparison of data for gasdynamic and electron microscope monitoring (see Table 2) indicates quite good conformity of them (difference ~10%). An exception is specimen 2 in the unloaded condition. In this case the gasdynamic pore radius is less than the electron microscope radius by a factor about 1.5. This difference is most probably caused by the annular nature of inlets for PETP-membrane pores [9]. The ratio of gas flows through a membrane before and after loading may also give information about the change in pore radius. The Knudsen equation for relative gas flow rate  $Q^*$  through  $N$  channels of an atomic membrane is written as

$$Q^* = \frac{2}{3} \frac{\pi R_p^3}{L} v_t N \quad (2)$$

( $v_t$  is average thermal velocity of gas molecules). If during loading, new pores do not arise in the membrane ( $N = nS = \text{const}$ ) and only existing pores expand, then the cubic root of the ratio of relative gas flow rate after loading  $Q^*$  to relative flow rate measured before loading  $Q_0^*$  should be equal to the ratio of average pore radius for a loaded specimen  $R_p$  to that of an unloaded specimen  $R_{p0}$ . In fact, as can be seen from Table 3, test ratio  $R_p/R_{p0}$  found using Eq. (2) agrees with an accuracy up to 2% with the similar value obtained from direct determination of  $R_p$  by the gasdynamic method. This also confirms the fact that the main reason for a sharp increase in freely molecular relative flow rate is an increase in pore radius and occurrence of new pores.

The authors thank Academician G. N. Flerov for support and interest in this work; also, O. L. Orelovich for help rendered.

#### LITERATURE CITED

1. G. N. Flerov, "Synthesis of superheavy elements and use of atomic physics methods in related fields," Vestn. Akad. Nauk SSSR, No. 4 (1984).
2. L. S. Palatnik, P. G. Cheremskoi, and M. Ya. Fuks, Pores in Films [in Russian], Énergoizdat, Moscow (1982).
3. V. I. Kuznetsov, V. V. Ovchinnikov, et al., "Gasdynamic determination of pore radius for membranes of the cellular type," Inzh.-Fiz. Zh., 4, No. 2 (1983).
4. V. E. Gul' and V. N. Kuleznev, Structure and Mechanical Properties of Polymers [in Russian], Vysshaya Shkola, Moscow (1966).
5. A. A. Askadskii, Deformation of Polymers [in Russian], Khimiya, Moscow (1973).
6. V. E. Gul' and V. P. D'yakonova, Physicochemical Bases for the Production of Polymer Films [in Russian], Vysshaya Shkola, Moscow (1978).
7. L. D. Landau and E. M. Lifshits, Elasticity Theory [in Russian], Nauka, Moscow (1965).
8. S. F. Borisov, B. A. Kalinin, et al., "Micromanometer with a digital counter," Prib. Tekh. Éksp., No. 4 (1972).
9. O. E. Aleksandrov, V. D. Seleznev, V. V. Ovchinnikov, et al., "Study of the evolution of the inlet profile of atomic membrane pores," Preprint No. P7-87-597, OIYaI, Dubna (1987).